Available online at www.sciencedirect.com
SCIENCE DIRECT
Biochemical Pharmacology 70 (2005) 90–101
Biochemical Pharmacology
www.elsevier.com/locate/biochempharm

Site specific alterations of adipose tissue mitochondria in 3′-azido-3′-deoxythymidine (AZT)-treated rats: An early stage in lipodystrophy?

Catherine Deveaud [a,*], Bertrand Beauvoit [b], Stéphanie Hagry [a], Anne Galinier [c], Audrey Carrière [c], Bénédicte Salin [a], Jacques Schaeffer [a], Sylvie Caspar-Bauguil [c], Yvette Fernandez [c], Jean-Baptiste Gordien [d], Dominique Breilh [d], Luc Penicaud [c], Louis Casteilla [c], Michel Rigoulet [a]

[a] *Institut de Biochimie et de Génétique Cellulaires, UMR 5095 CNRS-Université Victor Ségalen, 1 rue Camille Saint Saëns, 33077 Bordeaux Cedex, France*
[b] *INSERM U441, Avenue du Haut Lévêque, 33600 Pessac, France*
[c] *UMR 5018 CNRS-UPS, IFR31, Bât L1, CHU Rangueil, 31059 Toulouse Cedex 09, France*
[d] *Laboratoire de Pharmacocinétique et Clinique EA 525, Université Victor Ségalen, Hôpital Haut-Lévêque CHU Bordeaux, France*

Received 16 November 2004; accepted 11 April 2005

Abstract

Although it is well accepted that treatment with nucleoside reverse transcriptase inhibitors (NRTIs) modifies fat metabolism and fat distribution in humans, the mechanisms underlying these modifications are not yet known. The present investigation examines the effects of chronic oral administration of 3′-azido-3′-deoxythymidine (AZT) on the mitochondrial metabolism and the redox status management of rat white adipose tissues originating from two anatomical sites, as well as of the rat liver. Results showed that AZT treatment induced differential effects on the mitochondrial functions depending on the anatomical localisation. Indeed, in inguinal adipose tissue, a significant decrease in the cytochrome *c* oxidase activity and in the mitochondrial DNA (mtDNA) content was observed, whereas the activity of citrate synthase, a mitochondrial protein exclusively encoded by the nucleus, was not affected. In contrast, no significant change in these parameters could be detected for epididymal tissue and for liver. In parallel, no oxidative stress could be detected after treatment, for both white adipose tissues and for liver, even though treated liver exhibited several modifications in redox management. Taken together, these data demonstrate differential mitochondrial effects of AZT on subcutaneous versus visceral white adipose tissue. Moreover, the decrease in mitochondrial oxidative capacity of inguinal adipocyte consecutive to AZT treatment is not primarily due to an oxidative stress per se, but rather to a depletion of the mtDNA content per cell.
© 2005 Elsevier Inc. All rights reserved.

Keywords: Adipocyte; AZT; Lipodystrophy; MtDNA; Respiratory complexes; Reactive oxygen species (ROS)

1. Introduction

Protease inhibitors (PI) in combination with nucleoside reverse transcriptase inhibitors (NRTIs) are now considered to be the standard of care for optimal antiretroviral therapy for HIV infected patients. This kind of therapy, called HAART (for highly active anti retroviral therapy) has demonstrated clinical, immunological and survival benefits. However, with their widespread use the previously unrecognized side-effects are becoming more evident as drug availability improves and treatment duration increases. A syndrome combining peripheral fat wasting (affecting facial fat pads, arms and legs), insulin resistance and hyperlipidaemia, collectively referred to as lipodystrophy syndrome, has been identified in HIV-infected patients receiving this treatment [1]. The surprising feature of lipodystrophy syndrome is a difference in sensitivity to HAART between visceral and subcutaneous adipose tissues. In fact, under

Abbreviations: AUC, area under the curve; AZT, 3′–azido-3′–deoxythymidine; CCCP, carbonyl cyanide m-chlorophenylhydrazone; GPx, glutathione peroxidase; HAART, highly active anti retroviral therapy; MDA, malondialdehyde; mt DNA, mitochondrial DNA; nDNA, nuclear DNA; NRTI, nucleoside reverse transcriptase inhibitor; ROS, reactive oxygen specie; SOD, superoxide dismutase

* Corresponding author. Tel.: +33 5 56 99 90 40; fax: +33 5 56 99 90 40.
E-mail address: Catherine.Deveaud@wanadoo.fr (C. Deveaud).

0006-2952/$ – see front matter © 2005 Elsevier Inc. All rights reserved.
doi:10.1016/j.bcp.2005.04.015

HAART, subcutaneous adipose tissue is described as atrophying whereas visceral adipose tissue does not have this quality [2,3]. Although it was originally believed to be secondary to the use of the protease inhibitor class, it is now clear that NRTIs are also involved in this syndrome [4]. NRTIs are tri-phosphorylated by intracellular kinases. Although these triphosphorylated molecules preferentially inhibit HIV reverse transcriptase, they are also able to inhibit mitochondrial enzymes such as adenylate kinase, ADP/ATP translocase and the mitochondrial DNA polymerase gamma [5,6], the latter inhibition resulting in impaired synthesis of mitochondrial enzymes that are involved in oxydative phosphorylation [6].

It has been described that 3′-azido-3′-deoxythymidine (AZT) treatment could induce an oxidative stress in muscle [7], in liver [8] and in heart [9]. In fact, the redox metabolism brings together production and regulation mechanisms of reactive oxygen species (ROS). Basal production of ROS is required for cellular function. However, in order to regulate excessive production of ROS, cells contain combined anti-oxidant defences, namely enzymatic (e.g. superoxide dismutases (SODs), catalase, glutathione peroxidase (GPx)) and non enzymatic (α-tocopherol, Vitamin C, glutathione, coenzyme Qs) molecules. When these synergistic defences are overwhelmed, oxidative damage of essential structural and functional molecules such as DNA, carbohydrates, polyunsaturated fatty acids and proteins may appear. This corresponds to the oxidative stress which is also able to induce mitochondrial defects (for review see [10]).

The aims of this study were: (i) to determine whether a decrease in mitochondrial DNA content and/or an induction of oxidative stress in white adipose tissues, both capable of generating mitochondrial defects, were associated to AZT treatment in rats and (ii) to compare AZT effects on mitochondrial metabolism and redox parameters on subcutaneous and visceral white adipose tissues. To distinguish the effects of NRTIs from the others, we chose to treat rats with AZT because this molecule is the most widely used drug in acquired immunodeficiency syndrome (AIDS) therapy. Inguinal and epididymal tissues were chosen, respectively, as subcutaneous and visceral adipose tissue because they represent the two main lipid storage sites of rat fat pads [11]. Moreover, mitochondrial metabolism and anti-oxidant defences of hepatocytes were also evaluated in control and AZT-treated rats since it is well known that the liver is widely implicated in lipid metabolism.

2. Materials and methods

2.1. Animal care

Animal experimentation was performed according to the Helsinki convention for animal care and use. Male Wistar rats weighing 300 ± 10 g (Charles River Laboratories, l′Arbresle, France) were housed at 22 ± 2 °C, on a 12:12-h photoperiod, and were provided with food and water ad libitum. At the end of the first week, the animals were randomly divided into two groups. The AZT-treated group ($n = 10$) received AZT in their drinking water while the control group ($n = 9$) continued to receive plain tap water, both at libitum. The dose of AZT used here in drinking water was 0.6 mg/mL equivalent to 70 mg/kg body weight/day. This dose corresponds to human treatment regimens, i.e. 8–12 mg/kg/day, or 50–75 mg/kg/day in rats, after correction for the five- to seven-fold higher metabolic and drug disposal rate in rats compared with humans [12]. We chose a 1-month period of exposure because it has been previously used by investigators [13,14].

Water consumption of all rats was recorded daily thus allowing the calculation of the overall daily dose of AZT. The AZT solution was made up every day. All animals were weighed daily and their overall appearance and activity level noted at that time.

Before sacrifice, animals were anesthetized with 100 mg/kg ketamine and 10 mg/kg xylazine, mixed just before administration and they were bled from the posterior vena cava by drawing 3 ml of blood on heparin sodium.

2.2. Determination of blood pyruvate, lactate, β-hydroxybutyrate and acetoacetate

To remove proteins, 1 ml of 2 M perchloric acid, 25 mM EDTA was immediately added to 2 ml of blood on ice. The denatured material was precipitated by centrifugation at 2000 × *g* for 15 min, and the supernatant was neutralized with 2 M KOH, 0.3 M MOPS and was used to measure enzymatically pyruvate, lactate, β-hydroxybutyrate and acetoacetate as described [15].

2.3. Determination of plasma AZT concentration

Four rats received AZT in their drinking water at a concentration of 0.6 mg/ml (70 mg/kg/day). The estimated daily water consumption per rat was approximately 112 ± 8 ml/kg/day and occurred for 90% between 6 p.m. and 6 a.m and 10% between 6 a.m. and 6 p.m. Rats were sacrified at different times of the day (i.e. 4 a.m., 10 a.m., 5 p.m. and 11 p.m.). Before sacrifice, animals were anesthetized and they were bled from the posterior vena cava by drawing 3 ml of blood on heparin sodium. Plasma AZT concentrations were measured using the HPLC method with a C18 column (Prontosil-AQ+). The mobile phase was 10 mM potassium phosphate buffer (pH 3.5) and 20% acetonitrile. The detection limit in plasma was 5 ng/ml. The coefficients of variation were 5.1 and 7.4% for intra and interday, respectively. Plasma AZT concentrations were analyzed by a naïve pooled method by using a pharmacokinetic one-compartment model with elimination from the central compartment.

2.4. Tissue isolation

Two regions of adipose tissue were carefully dissected: the epididymal tissue, by a horizontal cut above the epididymus; and the inguinal subcutaneous tissue, by carefully dissecting all fat in the inguinal region up to a horizontal line parallel to the xyphoid cartilage. Tissues were dissected from visible blood vessels. Liver was also collected. Tissues were washed in phosphate buffered saline (PBS) medium, blotted, weighed and immediately frozen in liquid nitrogen. Aliquots were pulverized with a stainless steel mortar and pestle in liquid nitrogen. Powdered tissues were stored at −80 °C until use. For mitochondrial isolation and oxygen consumption, freshly isolated livers were used.

2.5. Microscopic analysis

Freshly dissected inguinal and epididymal adipose tissues as well as liver were fixed in glutaraldehyde 2.5% (v/v) in phosphate buffer (0.1 M, pH 7.2), postfixed in 1% (w/v) OsO_4, postfixed in uranyl acetate 1% (w/v), embedded in araldite and prepared for electron microscopy. Ultra-thin sections of adipose tissue were examined with a Philips Tecnai 12 Biotwin transmission electron microscope.

2.6. Isolation of liver mitochondria and measurement of oxygen consumption

Liver mitochondria were prepared using Klingenberg et al.'s basic isolation method [16] in a medium consisting of 250 mM sucrose, 1 mM EGTA and 20 mM Tris–HCl (pH 7.2). In short, the protocol consists of a homogenisation of the liver carried out using a motor-driven Teflon pestle homogenizer, and two subsequent differential centrifugation cycles (each cycle being a 700 × *g* centrifugation of the homogenate for 10 min followed by a 7000 × *g* centrifugation of the supernatant for 10 min). One additional centrifugation cycle has been added at the end of the protocol to improve the purity of the isolated mitochondrial fraction. All isolation steps were performed at 4 °C. Mitochondrial proteins were determined by the Biuret method, using bovine serum albumin as a standard.

The oxygen consumption of isolated mitochondria was measured polarographically at 37 °C using a Clark-type large diameter Orbisphere oxygen electrode in a 2 ml thermostatically controlled chamber (Oroboros Oxygraph, Paar, Graz, Austria). Data were recorded at sampling intervals of 1 s (DatLab Acquisition software, Oroboros, Innsbruck, Austria). Respiratory rates (J_0), i.e. rates of oxygen consumption, expressed as nanomoles of O atoms consumed per min and per mg mitochondrial protein (nat.O/min/mg mito prot), were determined from the slope of a plot of O_2 concentration versus time, divided by the biomass concentration. Isolated mitochondria (0.15 mg protein/ml) were incubated in the following buffer: 250 mM sucrose, 1 mM EGTA, 5 mM KPi and 20 mM Tris–HCl (pH 7.2). Mitochondria were energized with either glutamate plus malate (5 mM each), providing electrons to complex I of the respiratory chain, or succinate (5 mM), feeding electrons into complex II. Respiration was measured after addition of 0.2 mM ADP (state 3 respiration) and after total consumption of ADP (state 4 respiration). CCCP (0.1 μM) was used to uncouple respiratory chain. The respiratory control ratio (RCR) was calculated as the rate of oxygen consumption in states 3–4.

2.7. Mitochondrial enzymatic assays

Powdered frozen tissues (200–300 mg) were homogenized in 1.5 ml of PBS using a 4 ml-glass–glass homogenizer (Kontes Glass Co. Vineland, NJ, 0.025 mm clearance). Tissue homogenates were exposed to ultrasound energy (110 W) for 15 s on ice. Adipose samples were then centrifuged for 5 min at 600 × *g* and delipidated by aspirating the top of the supernatant. Isolated liver mitochondria were used just as they were.

Citrate synthase (E.C. 2.3.3.1, formerly E.C. 4.1.3.7) was measured according to the procedure of Srere [17], and one unit (U) of citrate synthase was equal to the reduction of 1 μmol of 5-5′-dithiobis-2-nitrobenzoic acid per min. Cytochrome *c* oxidase (E.C. 1.9.3.1) activity was measured spectrophotometrically according to Rustin et al. [18] except that Lubrol [5% (v/v) final concentration] was added to homogenates prior to measuring cytochrome *c* oxidase activity. One unit of cytochrome *c* oxidase was equal to the oxidation of 1 μmol of ferricytochrome *c*/min. Tissue data were expressed as U/mg DNA and isolated mitochondria data were expressed as U/mg protein.

2.8. Enzymatic and non enzymatic antioxidants and lipid peroxidation

Powdered frozen tissues (100 mg) were solubilized in 2-propanol for detection of α-tocopherol and CoQ9 (reduced and oxidized forms) by reverse-phase HPLC with electrochemical detection [19] on the same run. An aliquot of powdered frozen tissues was homogenized in 3 mM EDTA, 154 mM KPi, pH 7.4 at the following concentrations: 10% (w/v) for liver and 50% (w/v) for inguinal and epididymal tissues. The homogenates were sonicated (30 s, 4 °C) and then centrifuged at 8000 × *g* for 10 min. Supernatants were centrifuged at 105,000 × *g* for 45 min, 4 °C. Final supernatant was used for protein, antioxidant enzyme, other non enzymatic antioxidants (glutathione and Vitamin C) and lipid peroxidation assays.

SOD activity (Mn SOD and Cu/Zn SOD) were assayed by using the inhibition of pyrogallol autoxidation [20]. One unit (U) of SOD activity was defined as the amount of enzyme that inhibited pyrogallol autoxidation by 50%. Catalase activity was determined by measuring decomposition of H_2O_2 at 240 nm [21]. GPx activity was

measured using *t*-butylhydroperoxide as substrate [22]. One unit of GPx activity corresponds to the oxidation of 1 μmol of NADPH/min.

After precipitation of proteins: (i) reduced form of glutathione and oxidized one were detected by reverse-phase HPLC with electrochemical detection [23]; (ii) total Vitamin C and oxidized form were detected by reverse-phase HPLC with fluorimetric detection [24] using two different runs. The reduced form was calculated by subtracting the oxidized from total Vitamin C. For CoQ9, glutathione and Vitamin C, the percentage of oxidized form was calculated as [oxidized form × 100/(oxidized + reduced) forms].

Lipid peroxidation was estimated from the formation of malondialdehyde (MDA) by a spectrofluorimetric method [25].

2.9. DNA quantification

Powdered frozen tissues (200–300 mg) were homogenized in 1.5 ml of PBS as described for mitochondrial enzymatic assays.

Total DNA was quantified from delipidated tissue homogenates using the method of Labarca and Paigen [26]. This method takes advantage of the fluorescence enhancement of DNA-dye complex produced after the specific interaction of total cellular DNA with fluorescent dye (Hoescht H33258, Sigma). DNA content for each sample was extrapolated from a standard curve constructed using 0–1 μg/ml of calf thymus DNA (Sigma).

2.10. DNA extraction and mtDNA quantification

Total DNA was extracted from tissue powder using proteinase K followed by a purification step using Nucleospin Tissue kit (Macherey Nagel) according to the manufacturer's instructions. Total DNA was digested with *Bam*H1 overnight at 37 °C. DNase-free RNase was added to this digestion in order to eliminate RNA. DNA probes were generated by PCR from total DNA isolated from rat liver and purified after electrophoresis using a QIA quick gel extraction kit (Qiagen). For quantitative assessment of mtDNA, 50–200 ng of total DNA were denatured by heating at 100 °C for 5 min. It was then diluted 10-fold in 0.4 M NaOH, 10 mM EDTA and dotted onto nylon + - membrane (Hybond XL, Amersham) using a Bio-Dot microfiltration apparatus (Hoefer PR 648 Filtration Manifold). mtDNA was detected by using a PCR fragment of mtDNA. The amount of total cellular DNA loaded on the membrane was standardized with a PCR fragment of 18S gene. cDNA probes were radiolabeled by synthesis of uniformly labeled DNA probes using random oligonucleotide primers (kit from GIBCO BRL) with ^{32}P-labeled dCTP nucleotides (Amersham), so that their final activities were between 1 and 4×10^8 cpm/mg. The blots were prehybridized for 4 h at 68 °C in a solution containing 5 SSC (standard saline citrate), 5 × Denhardt, 1% SDS and 0.1 mg/ml denatured salmon sperm DNA. The filters were then hybridized overnight at 68 °C in the same solution plus an excess of the cDNA probes (10^6 cpm/ml). The blots were then washed twice 15 min at room temperature in 2 SSC and twice 30 min at 55 °C in 0.1 SSC and 0.1% SDS. The filters were exposed to X-ray films at −70 °C using intensifying screens. DNA slot-blots were quantified by radioactive scanning (PhosphoImager, Molecular Dynamics, ImageQuant). The amount of mtDNA was determined as the ratio of the mtDNA probe radioactive signal to the 18S probe radioactive signal (nDNA).

2.11. Statistical analysis

The results are expressed as the mean ± S.E.M. Statistical analysis was carried out using non-parametric Mann–Whitney (Statsdirect, UK). A probability value of less than 0.05 was considered significant.

3. Results

3.1.1. Physiological characteristics of AZT treated rats

AZT was administered in drinking water rather than by gavage or by injection. The estimated daily water consumption per rat was not significantly different over the 4-week period averaging 119 ± 8 and 109 ± 10 ml/kg/day for control and AZT-treated rats, respectively. Thus, the AZT-treated rats were treated with 70 mg/kg/day for 1 month. The plasma concentration time data for AZT were analyzed using a pharmacokinetic one-compartment model with elimination from the central compartment. Considering oral bioavailability (F) of AZT equivalent to 90% in rats as referred by Hasegawa et al. [27], the total AUC in our rats was obtained by adding $AUC_{6\ p.m.-6\ a.m.}$ (90% water consumption) with $AUC_{6\ a.m.-6\ p.m.}$ (10% water consumption) and was equal to 872 μg min/ml. The total body clearance (CL_T/F) was 26 ml/min and the apparent volume of distribution (Vd/F) was 1.73 ml (with elimination half-life $T_{1/2Ke}$ = 15 min). Our method of AZT administration was not the usual method (drinking water instead of gavage or injection) and did not allow us to make comparative analyses of our results with previous work by other authors. However, we chose this method because it limited animal stress which could interfere with energy metabolism.

Both the control and AZT-treated male rats gained weight steadily over the 4-week period of treatment and no significant differences existed in body weight gain between the two groups during the treatment (3.52 ± 0.37 and 3.09 ± 0.37 g/day for control and for AZT-treated rats, respectively). All animals appeared healthy and displayed comparable levels of alertness and activity when removed from their cages for weighing.

Table 1
Effect of AZT on blood metabolites[a]

	Lactate (mM)	Pyruvate (mM)	Lactate/pyruvate ratio	βOHbutyrate (mM)	Acetoacetate (mM)	βOHbutyrate/acetoacetate ratio
Control ($n = 6$)	1.32 ± 0.14	0.14 ± 0.02	9.56 ± 0.91	0.42 ± 0.03	0.22 ± 0.02	1.95 ± 0.12
AZT-treated ($n = 4$)	1.46 ± 0.42	0.17 ± 0.04	8.66 ± 0.49	0.53 ± 0.13	0.20 ± 0.04	$2.63 \pm 0.13^{*}$

[a] Asterisk indicates significant differences between control and AZT-treated rats ($^{*}p < 0.05$; Mann–Whitney test). Metabolites were measured enzymatically in blood as described in Section 2.

The administration of AZT to rats for 4 weeks had no significant effect on the weight of inguinal (6.5 ± 0.5 and 6.8 ± 0.4 g for control and AZT-treated, respectively), nor epididymal (6.00 ± 0.1 and 6.4 ± 0.8 g for control and AZT-treated, respectively) adipose pads of rats weighing about 410 ± 10 g.

3.2. Blood level of pyruvate, lactate, β-hydroxybutyrate and acetoacetate

After measure of lactate, pyruvate, β-hydroxybutyrate and acetoacetate concentrations, lactate/pyruvate and β-hydroxybutyrate/acetoacetate ratios were calculated (Table 1). From an energy point of view, these ratios are extremely important because they, respectively, reflect the cytoplasmic redox state (i.e. $NADH_{cyt}/NAD^{+}_{cyt}$) and the mitochondrial redox state (i.e. $NADH_{mito}/NAD^{+}_{mito}$) of hepatocytes [28]. Although the blood levels of lactate, pyruvate and β-hydroxybutyrate were slightly increased in AZT-treated rats, they were not significantly different from the control. In the same way, the level of acetoacetate was not modified in AZT-treated rats. While the lactate/pyruvate ratio was slightly decreased in AZT-treated rats, it was not significantly different from the control. In contrast, the β-hydroxybutyrate/acetoacetate ratio was significantly higher in AZT-treated than in control rats (2.63 ± 0.13 versus 1.95 ± 0.12, $p < 0.05$).

3.3. Effects of AZT treatment on liver

3.3.1. Morphological characteristics

Since the blood β-hydroxybutyrate/acetoacetate ratio was significantly increased for AZT-treated rats, it could mean that mitochondrial redox state (i.e. $NADH_{mito}/NAD^{+}_{mito}$) of hepatocytes was altered. Examination of thin sections of liver obtained from AZT-treated rats revealed ultrastructural anomalies on electron microscopy (Fig. 1). The alterations detected were vacuolar degeneration and involved mainly the rough endoplasmic reticulum (RER). Mitochondrial structures were unremarkable.

3.3.2. Liver redox metabolism parameters

It is worth noting that each enzymatic activity was expressed per mg of total DNA (cellular parameter) rather than per mg of total protein or per g of wet weight tissue (tissular parameters). Therefore, this normalization made it possible to compare enzymatic activity per cell which will be particularly useful when comparing data on two types of adipose tissue cell. For consistency, enzymatic activities were also expressed per mg of total DNA for liver.

For control liver, enzymatic activities were: 1146 ± 113 U/mg DNA (Cu/Zn SOD), 72.7 ± 2.2 U/mg DNA (GPx) and $16{,}600 \pm 2600$ U/mg DNA (catalase). α-Tocopherol and total CoQ9 amounts were 15.1 ± 1.6 and 67.1 ± 7.2 μmol/mg DNA, respectively. The percentage of oxidized CoQ9 was 5.6 ± 1.6. These redox parameters were not significantly modified by AZT treatment. However, it is notable that Mn SOD activity was two-fold higher than for control rats (252.9 ± 34.3 U/mg versus 117.2 ± 40.0 U/mg DNA). Moreover, Fig. 2 showed that the liver of AZT-treated

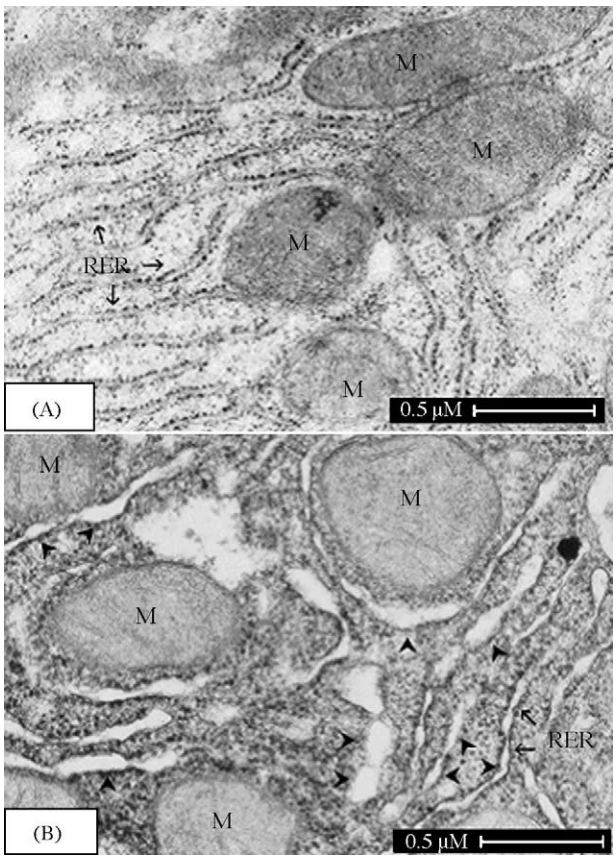

Fig. 1. Representative electron micrographs of liver section. Tissue fixation and thin sections were prepared as described in Section 2 from control rats (A) and AZT-treated rats (B). M: mitochondria, RER: rough endoplasmic reticulum. No ultrastructural anomalies were detected in the organization of mitochondria. However, arrows (→) indicated abnormal dilatations on the RER of AZT-treated rat (B).

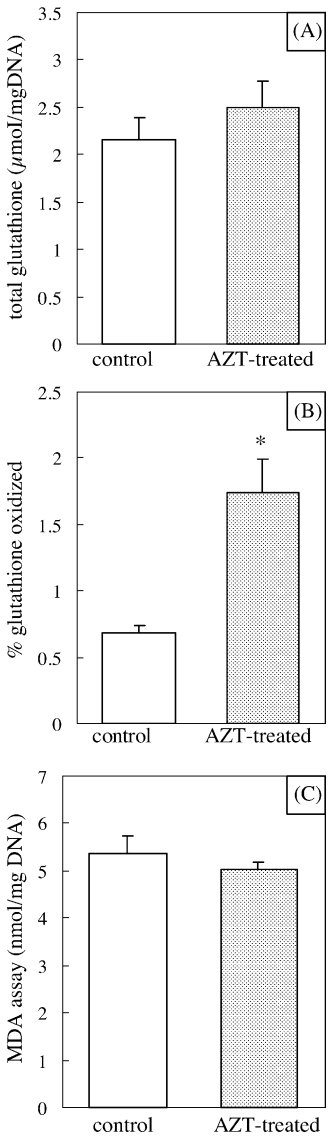

Fig. 2. Effect of AZT on total glutathione, glutathione redox state and MDA level in liver. Oxidized and reduced forms of glutathione were measured as described in Section 2 by HPLC with electrochemical detection and used for the quantification of total (A) and percentage oxidized glutathione (B). MDA (C) was measured by spectrofluorimetry as described in Section 2. Values are mean ± S.E.M. of independent determinations on six rats. Asterisks indicate significant differences between control and AZT-treated tissue ($^{*}p < 0.05$).

rats had a significantly higher percentage of oxidized glutathione than the controls without modification of total glutathione amount. Significant ($p < 0.05$) higher percentage of oxidized Vitamin C was observed in AZT-treated rat livers (14.3 ± 1.8) compared to controls (9.9 ± 1.0) without modification of total Vitamin C (not shown). MDA measurement such as the lipid peroxidation index was not significantly different between AZT-treated and control rats (Fig. 2C).

3.3.3. Liver mitochondrial metabolism

The specific activity of three enzymes belonging to the respiratory chain and located in the inner mitochondrial membrane, namely succinate-dehydrogenase (complex II), cytochrome *c*–coenzyme Q oxydoreductase (complex III) and cytochrome *c* oxidase (complex IV) as well as the specific activity of citrate synthase, an enzyme located in the mitochondrial matrix which is usually used as an index of the mitochondrial mass, was measured on isolated liver mitochondria (Table 2). No significant difference could be detected in liver mitochondrial enzymatic equipment between AZT-treated and control rats.

Table 2
Effect of AZT on enzyme profiles of isolated liver mitochondria[a]

(U/mg prot)	Control ($n = 4$)	AZT treated ($n = 4$)
Succinate dehydrogenase	0.055 ± 0.03	0.054 ± 0.01
Cytochrome *c*–coenzyme Q oxido-reductase	0.57 ± 0.19	0.58 ± 0.12
Cytochrome *c* oxidase	3.0 ± 1.13	4.0 ± 0.25
Citrate synthase	0.16 ± 0.06	0.16 ± 0.03

[a] Specific activities were measured at 37 °C as described in Section 2. 1 unit is the amount of enzyme catalyzing the transformation of 1 μmol of substrate/min.

To determine whether the functional properties of the respiratory chain complexes were in accordance with the mitochondrial enzymatic equipment, mitochondrial respiration was assessed on isolated liver mitochondria. Different steady states were analyzed, namely ATP synthesis (addition of ADP) or not (no ADP addition), uncoupling (addition of CCCP) which made it possible to measure the coupling of oxidative phosphorylations and the maximal respiratory capacity. Under all these conditions, different substrates were used: glutamate plus malate or succinate (Table 3). Regardless of the steady state, no significant difference in the rate of respiration could be detected between mitochondria isolated from AZT-treated and control rats. This means that liver mitochondria from both origins have comparable oxidative phosphorylation capacities.

As shown above, AZT did not modify liver mitochondrial enzymatic equipment per se, nor did it alter mitochondrial oxidative phosphorylation functionality. However, to make sure that mitochondrial enzymatic equipment per cell was not decreased in AZT-treated rats, the specific activity of succinate-dehydrogenase and cyto-

Table 3
Effect of AZT on oxygen consumption of isolated liver mitochondria[a]

	Control ($n = 6$)		AZT-treated ($n = 7$)	
	Glutamate + Malate	Succinate	Glutamate + Malate	Succinate
Basal (state 4)	7.7 ± 0.5	19.9 ± 1.5	6.9 ± 0.8	16.7 ± 2.2
ADP (state 3)	67.7 ± 6.4	77.8 ± 8.4	66.6 ± 6.9	66.3 ± 6.2
CCCP	72.2.0 ± 6.0	99.8 ± 13.5	72.3 ± 5.6	85.5 ± 5.5
RCR	9.2 ± 1.1	3.9 ± 0.5	10.4 ± 1.4	4.3 ± 0.6

[a] Mitochondria isolation and oxygen consumption measurements were performed as described in Section 2. Oxygen consumption rate was expressed as nat O/min/mg proteins. Respiratory control ratio (RCR) is defined as the rate between the respiratory rate measured as state 3 versus state 4.

Table 4
Effect of AZT on enzyme profiles of liver[a]

(U/mg DNA)	Control ($n = 4$)	AZT treated ($n = 4$)
Succinate dehydrogenase	0.39 ± 0.02	0.37 ± 0.01
Cytochrome *c* oxidase	90 ± 12	106 ± 10
Citrate synthase	3.52 ± 0.34	4.77 ± 1.1

[a] Specific activities were measured at 37 °C as described in Section 2. 1 unit is the amount of enzyme catalyzing the transformation of 1 μmol of substrate/min.

chrome *c* oxidase, as well as citrate synthase was measured on liver homogenates (Table 4). Specific activities of succinate-dehydrogenase and cytochrome *c* oxidase were not significantly changed by AZT treatment. Although specific activity of citrate synthase was slightly increased in AZT-treated rat liver, it was not significantly different from the control.

3.4. Effects of AZT treatment on inguinal and epididymal adipose tissues

3.4.1. Cellularity and morphological characteristics

Inguinal and epididymal adipose tissue cellularity was assessed by measuring total DNA in delipidated tissue homogenates. AZT treatment did not change the cellularity of the inguinal adipose tissue (500 ± 90 μg versus 518 ± 90 μg DNA/g wet weight) nor that of epididymal tissue (136 ± 16 μg versus 140 ± 29 μg DNA/g wet weight).

Thin sections of inguinal and epididymal adipose tissues obtained from control and AZT-treated rats were examined on electron microscopy (Fig. 3). The alterations detected in both tissues from AZT-treated rats were vacuolar degeneration and mainly involved the rough endoplasmic reticulum (RER). Alterations detected by electron microscopy in liver and adipose tissues from AZT-treated rats were similar. These alterations were also described by Corcuera et al. [14] who found dilatation of the RER in the liver and the myocardium of rats treated with AZT (90 mg/kg/day) for thirty days. These authors also described the presence of autophagic vacuoles in the mitochondria. We could not detect any ultrastructural alteration in mitochondria. However, this could be explained by the fact that our AZT treatment was weaker.

3.4.2. Mitochondrial enzymatic equipment

The specific activity of several mitochondrial enzyme markers was measured on adipose tissue homogenates (Fig. 4A). Cytochrome *c* oxidase activity was significantly decreased in inguinal adipose cells of AZT-treated rats (4.43 ± 0.94 U/mg versus 8.28 ± 1.13 U/mg DNA, $p < 0.05$). In contrast, it was not significantly modified in epididymal adipose cells of AZT-treated rats (Fig. 4A). Moreover, the specific activity of citrate synthase was not significantly affected by AZT treatment whichever type of adipose tissue was considered (Fig. 4B).

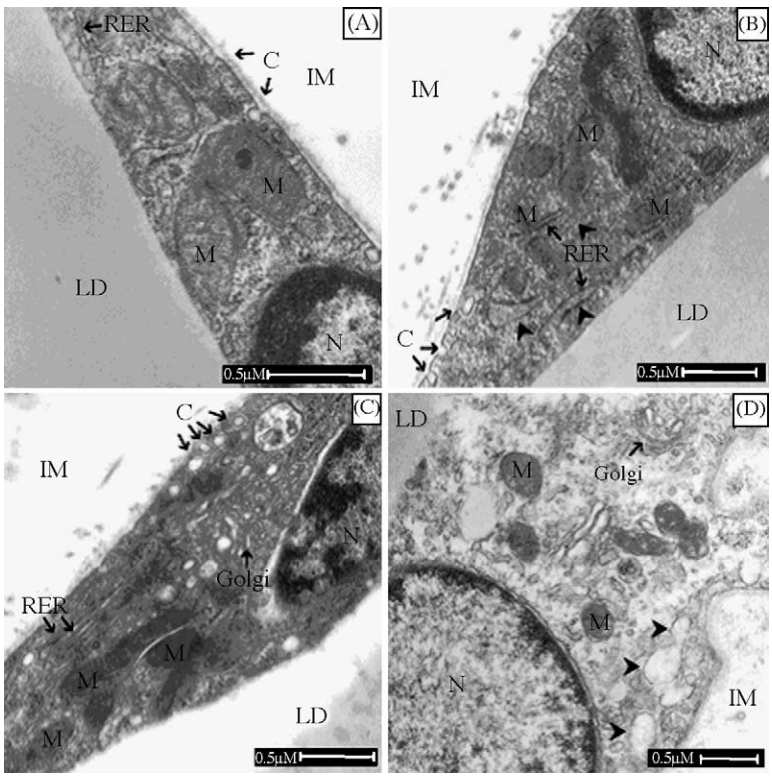

Fig. 3. Representative electron micrographs of inguinal and epididymal adipose tissue sections. Tissue fixation and thin sections were prepared as described in Section 2 from inguinal (A) and epididymal (C) from control rats and inguinal (B) and epididymal (D) from AZT-treated rats. IM: intercellular matrix, LD: lipid droplet, M: mitochondria, N: nucleus, RER: rough endoplasmic reticulum, C: caveole. Arrows (→) indicated abnormal dilatations on the RER of inguinal (B) and epididymal (D) tissues in AZT-treated rat.

3.4.3. Mitochondrial DNA content

Mitochondria have their own double-strand DNA molecule (mtDNA) encoding 13 proteins which constitute a portion of the four enzyme complexes involved in the oxidative phosphorylation system. To determine the mtDNA content of inguinal and epididymal adipose tissues, total DNA was analyzed by slot-blot hybridization using ^{32}P-labeled cDNA specific for mtDNA. The quantity of DNA loaded on the membrane was normalized using the18S cDNA probe. These cDNA probes used for detecting mtDNA and nDNA were suitable since they were exclusively specific to either mtDNA or 18S DNA, respectively [29]. The densitometric and normalized quantifications are represented on Fig. 4C. Inguinal adipose tissue of AZT-treated rats contained significantly less mtDNA than that provided from control animals (1.91 ± 0.20 versus 2.70 ± 0.22, $p < 0.05$). On the other hand, no significant difference of mitochondrial DNA content in epididymal cells from AZT and control rats could be detected (Fig. 4C).

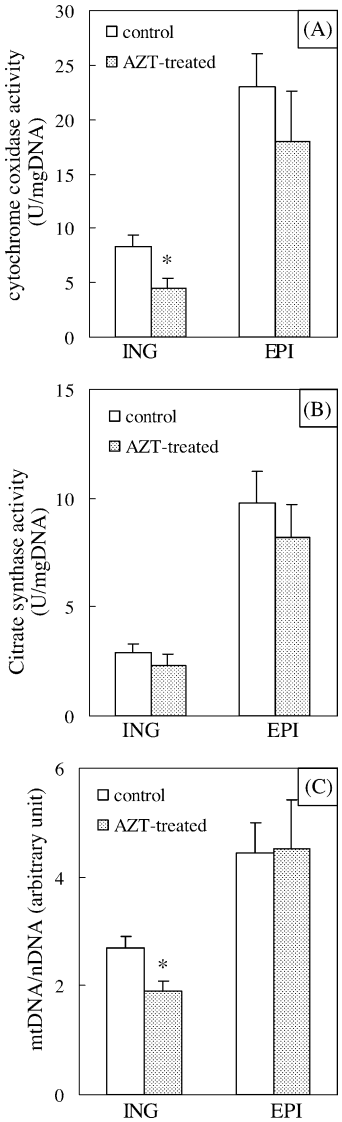

Fig. 4. Effect of AZT on enzyme profiles and mtDNA of inguinal and epididymal adipose tissues. Specific activities of cytochrome *c* oxidase (A) and citrate synthase (B) were measured in triplicate on homogenate as described in Section 2 in inguinal and epididymal tissues from control and AZT-treated rats. Values are mean ± S.E.M. of independent determinations on five rats. mtDNA content (C) was measured on isolated total DNA as described in Section 2 of inguinal and epididymal tissues from control and AZT-treated rats. Slot-blot autoradiograms were scanned densitometrically, values in the linear range were plotted against total DNA concentration and the slope was determined from linear regression analysis. All slopes were normalized with those generated by hybridization with the 18S gene. Values are mean ± S.E.M. of independent determinations on four rats. Asterisks indicate significant differences between control and AZT-treated rat, $^{*}p < 0.05$.

3.4.4. Correlation between cytochrome c oxidase and mtDNA

For control rats, a direct relationship between the cytochrome *c* oxidase activity and the mtDNA content of white adipose tissues has previously been shown [29]. This correlation thus indicated the importance of the number of mtDNA copies in determining the phenotype and more particularly the energy capacity of adipose cells. The question was therefore raised of this relationship in the adipose tissues of AZT-treated rats. Indeed, for each individual measurement carried out on inguinal and epididymal tissues of control and AZT-treated rats, the specific cytochrome *c* oxidase activity was plotted against the mtDNA level of the respective tissue (Fig. 5). A high degree of correlation ($r^2 = 0.88$) between the specific cytochrome *c* oxidase activity and the mtDNA level was found, regardless of the type of white adipose tissue and of the category of rats (AZT-treated or control).

3.4.5. Redox metabolism parameters

For adipose tissue controls, α-tocopherol amounts (217 ± 19 and 374 ± 33 μmol/mg DNA in inguinal and in epididymal cells, respectively) were not significantly modified by AZT (results not shown). Enzymatic activities,

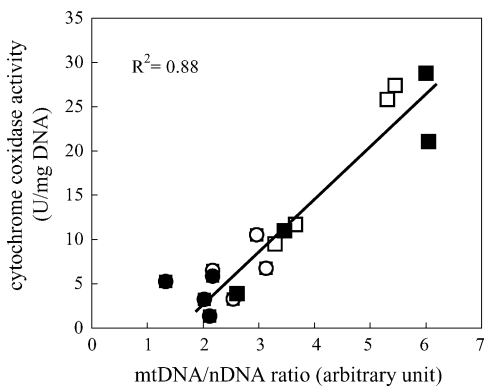

Fig. 5. Correlation between mtDNA level and specific activity of cytochrome *c* oxidase in inguinal and epididymal adipose tissues. Enzymatic assays were carried out in triplicate on each homogenate coming from inguinal (○) and epididymal (□) tissues of control rats and from inguinal (●) and epididymal (■) tissues of AZT-treated rats. Specific activities were plotted against the relative mtDNA content of the respective tissue. Correlation coefficient was $r^2 = 0.88$; $p < 0{,}0001$; $n = 16$.

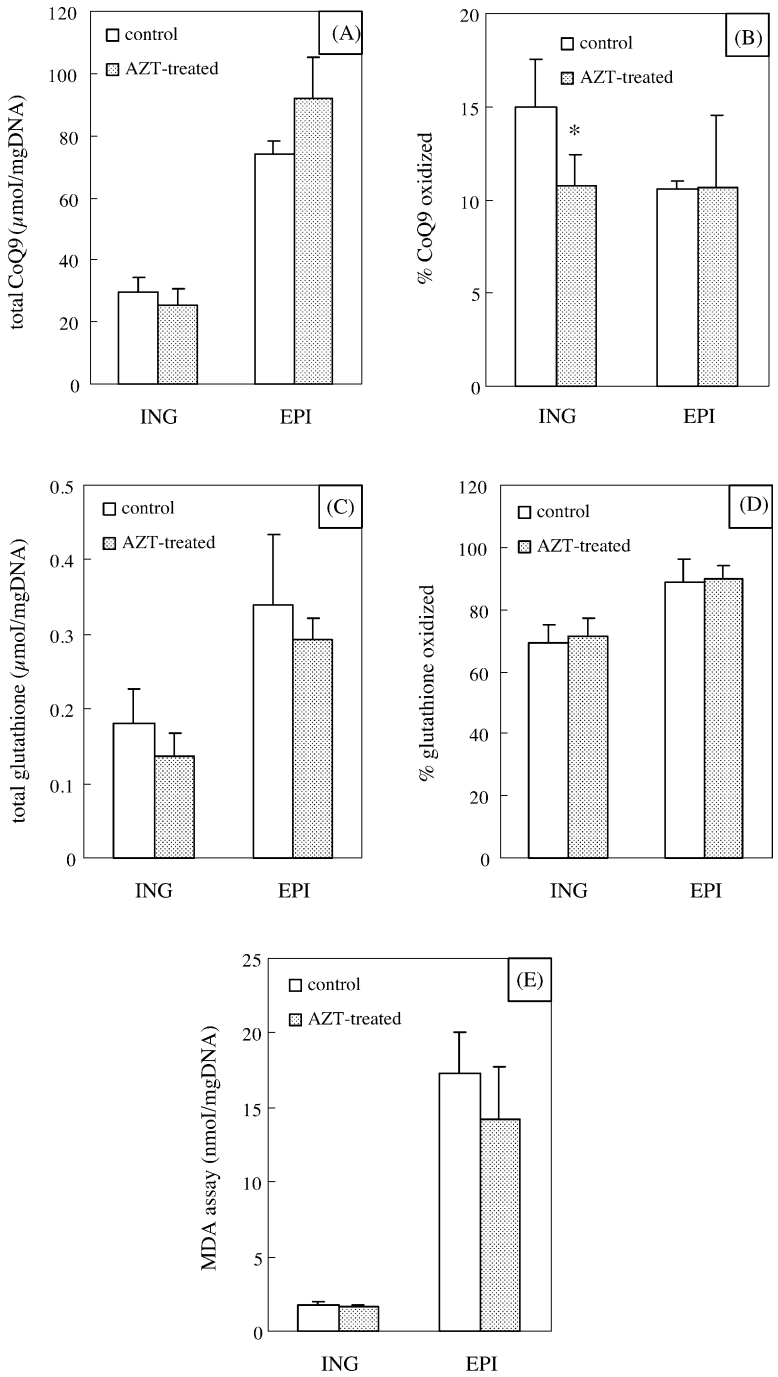

Fig. 6. Effect of AZT on total and percentage oxidized CoQ9, total glutathione, glutathione redox state and MDA in inguinal and epididymal adipose tissues. Oxidized and reduced forms of CoQ9 were measured as described in Section 2 by reverse-phase HPLC with electrochemical detection and used for the quantification of total (A) and percentage oxidized CoQ9 (B). Oxidized and reduced forms of glutathione were measured as described in Section 2 by HPLC with electrochemical detection and used for the quantification of total (C) and percentage oxidized glutathione (D). MDA (E) was measured by spectrofluorimetry as described in Section 2. Values are mean ± S.E.M. of independent determinations on six rats. Asterisks indicate significant differences between control and AZT-treated tissue ($^{*}p < 0.05$).

respectively in inguinal and epididymal tissue cells of controls were: 165 ± 86 U/mg versus 129 ± 19 U/mg DNA for Cu/Zn SOD, 5.2 ± 1.8 U/mg versus 20.2 ± 13.00 U/mg DNA for Mn SOD 3.7 ± 0.5 U/mg versus 9.5 ± 1.4 U/mg DNA for GPx and 310 ± 30 U/mg versus 940 ± 90 U/mg DNA for catalase. However, these enzymatic activities were not significantly different between controls and AZT-treated rats (results not shown). As shown in Fig. 6A, the total CoQ9 amount, higher in epididymal than in inguinal, was not significantly modified by AZT treatment. However, in inguinal tissue, the percentage of oxidized CoQ9 was significantly lower in AZT-treated than in control rats (Fig. 6B). Total glutathione and its percentage of oxidized form (Fig. 6C and D), were not

modified by AZT treatment. Similarly, lipid peroxydations probed using MDA, higher in epididymal than in inguinal tissue cells, were not modified by AZT (Fig. 6E).

4. Discussion

Although treatments with NRTIs can modify fat metabolism and fat distribution in humans, the mechanisms underlying these modifications and the respective role of each NRTIs is unknown. Moreover, these alterations are probably the consequence of several non exclusive factors, namely: HIV infection, protease inhibitors and NRTIs. To distinguish the effects of NRTIs from these other factors, we decided to treat rats with AZT, rather than other available drugs, as it is the best-known drug used in acquired immunodeficiency syndrome (AIDS) therapy. Adverse effects of AZT have been linked to mitochondrial toxicity. Two of the proposed mechanisms by which AZT interferes with mitochondrial functions is the depletion of mtDNA due to inhibition of DNA polymerase γ by triphosphorylated AZT [5,6] and/or oxidative stress due to an excessive production of ROS [7,8].

Therefore, this study set out: (i) to determine whether a decrease in mitochondrial DNA content and/or an induction of oxidative stress in liver and white adipose tissues, both capable of bringing about mitochondrial defects, were associated to AZT treatment in rats and (ii) to compare AZT effects on mitochondrial metabolism and redox parameters on subcutaneous and visceral white adipose tissues.

Under our conditions of treatment (i.e. 70 mg/kg/day for 1 month), the weight as well the cellularity of inguinal and epididymal adipose pads were not modified, which means that AZT, under our conditions, did not induce lipodystrophy in rats. Nevertheless, it is fair to think that metabolic anomalies induced by AZT may precede physical modifications. When these metabolic anomalies became overwhelming, clinical symptoms might appear. In this context, several parameters of energy metabolism were determined in different organs in order to detect early AZT-induced modifications.

Whereas lactate/pyruvate ratio in blood was not significantly modified by AZT, β-hydroxybutyrate/acetoacetate ratio increased by 35% for AZT-treated rats. These data are coherent with those obtained by Gaou et al. [30] who found that the same ratio was increased in d4T-treated mice fasted for 48 h. The β-hydroxybutyrate/acetoacetate ratio which reflected the mitochondrial NADH/NAD^+ ratio because of the equilibrium of mitochondrial β-hydroxybutyrate dehydrogenase [28] has been widely used to probe for mitochondrial dysfunctions of liver in animal studies [31]. One can deduce that liver mitochondria of AZT-treated rats were in a more reduced state than those of the controls. This redox state modification could be consistent with alterations of liver mitochondrial respiratory chain in AZT-treated rats. However, no significant difference in enzymatic equipment and functionality of liver mitochondria were detected between control and AZT-treated rats. These data suggest that increase in the mitochondrial NADH/NAD^+ ratio by treatment was due to changes in oxidative phosphorylation steady state rather than mitochondrial dysfunction per se. AZT treatment did not induce lipid-peroxidation, one of the markers of oxidative stress, in the liver. However, this treatment induced a significant increase in the percentage of glutathione and Vitamin C oxidized forms. This could be due to the accentuated consumption of their related reduced forms for ROS scavenging. Moreover, the large increase in Mn SOD activity should be a logical consequence of an increase in the production of mitochondrial superoxide anion [32]. This reveals that livers of AZT-treated rats exhibited modifications in redox metabolism management. In this context, liver may be fragilized with regard to possible oxidative stress, induced for instance by HIV invasion or opportunist infections.

The second part of this study was to compare effects of AZT in rat subcutaneous and visceral adipose tissues. Indeed, few studies have offered explanations for redistribution of adipose tissues. Fliers et al. [33] proposed that HIV associated lipodystrophy syndrome was mediated via the central nervous system and represented a selective neuropathy. Also, Giusti et al. [34] showed a different regulation of visceral and subcutaneous adipose tissues, suggesting a different role of both tissues in insulin resistance and lipid storage.

In our study, antioxidant defences were much weaker in adipose tissues than in liver, except for α-tocopherol. Moreover, the percentage of glutathione and CoQ9 oxidized forms were much higher in adipose tissues than in liver. Thus, under control conditions, the redox environment, as stated by the oxidized and reduced form of glutathione and CoQ9, was strongly oxidized in adipose tissues in comparison with the liver. This could be due not only to the weak amount of antioxidant defences but also to the strong level of peroxidable substrate (PUFA or polyunsaturated fatty acid amount) in adipose tissues.

In control rats, antioxidant defences were generally weaker in inguinal than in epididymal tissues, except for Cu/Zn SOD. In spite of that, the percentage of glutathione oxidized and MDA level were similarly weaker in inguinal than in epididymal tissues and were not modified by AZT treatment. This indicates that no oxidative stress could be detected in the two types of white adipose tissues in our conditions of treatment. Nevertheless, under the same conditions of treatment, AZT significantly decreased the mitochondrial DNA content of inguinal adipose cells but did not modify mitochondrial DNA content of epididymal adipose cells. Both results are consistent with the published data. In fact, it has been shown that lipodystrophy with peripheral fat wasting following treatment containing NRTIs was associated with a decrease in subcutaneous adipose tissue mtDNA content [35,36]. Moreover, NRTI

therapy was shown to be associated with a reduction of mtDNA content in subcutaneous fat, consistent with the hypothesis that NRTI-induced mtDNA depletion contributes to the pathogenesis of subcutaneous fat wasting [37,38]. In contrast, d4T or AZT treatment did not have any effect on epididymal adipose tissue mtDNA in mice [39]. One of the major results of this report is that AZT has specific effects on inguinal tissue and not on epididymal tissue. In our results, the decrease in mtDNA content per inguinal cell was correlated with a decrease in the cytochrome *c* oxidase activity and the percentage of oxidized CoQ9. These different modifications could reveal a decrease in the mitochondrial respiratory chain activity. Interestingly, a direct relationship was found between cytochrome *c* oxidase activity and mtDNA content of white adipose tissues, regardless of the treatment or not (Fig. 5) and of the anatomical location of the fat pad (Fig. 5 and see [29]). This correlation is in agreement with the fact that 3 over 13 subunits of cytochrome *c* oxidase are mitochondrially encoded. Since AZT-treatment decreased the activity of cytochrome *c* oxidase but not that of citrate synthase activity, a mitochondrial protein exclusively encoded by the nucleus, we can reasonably hypothesize that partial cytochrome *c* oxidase defect of inguinal adipose cells is a consequence of AZT-induced mtDNA depletion. The reason for this higher sensitivity to AZT in inguinal tissue as compared to epididymal tissue, which we have demonstrated, is open to question. However, since phosphorylated forms of AZT have structural similarity with ADP and ATP, they could be mimicking them to interact on some mitochondrial enzymes (i.e. ADP/ATP translocator, adenylate kinase, polymerase gamma (for review see [6]). In this case, it is possible that the higher sensitivity of inguinal tissue could be due to its weaker mitochondrial enzymatic equipment per cell (compared with epididymal) [29].

The other main result of this report is that, under our treatment conditions, AZT did not produce cell oxidative stress in both adipose tissues. Taken together, these data demonstrate that a decrease in mitochondrial oxidative activity consecutive to AZT treatment in adipose tissues is not linked primarily to oxidative stress but to a decrease of mtDNA. Therefore, it could be possible that oxidative stress detected in muscle, liver and heart after AZT exposition [7–9] may not be a cause but rather a consequence of the decrease in mitochondrial oxidative capacity.

Acknowledgments

The authors wish to thank Joanne Pageze for her contribution to the editing of the English manuscript and Jean-Marc Bernadou for his technical assistance in dosing the AZT concentrations in plasma. This work was supported by a grant from ANRS (Agence Nationale de Recherche sur le Sida). C.D. was a recipient of a grant from ANRS.

References

[1] Carr A, Samaras K, Burton S, Law M, Freund J, Chisholm DJ, et al. A syndrome of peripheral lipodystrophy, hyperlipidaemia and insulin resistance in patients receiving HIV protease inhibitors. AIDS 1998;12:F51–8.
[2] Carr A, Samaras K, Chisholm DJ, Cooper DA. Abnormal fat distribution and use of protease inhibitors. Lancet 1998;351:1736.
[3] Shaw AJ, McLean KA, Evans BA. Disorders of fat distribution in HIV infection. Int J STD AIDS 1998;9:595–9.
[4] Kakuda TN, Brundage RC, Anderson PL, Fletcher CV. Nucleoside reverse transcriptase inhibitor-induced mitochondrial toxicity as an etiology for lipodystrophy. AIDS 1999;13:2311–2.
[5] Brinkman K, Smeitink JA, Romijn JA, Reiss P. Mitochondrial toxicity induced by nucleoside analogue reverse transcriptase inhibitors is a key factor in the pathogenesis of antiretroviral therapy related lipodystrophy. Lancet 1999;354:1112–5.
[6] Barile M, Valenti D, Quagliariello E, Passarella S. Mitochondria as cell targets of AZT (zidovudine). Gen Pharmacol 1998;31:531–8.
[7] De la Asuncion JG, Del Olmo ML, Sastre J, Millan A, Pellin A, Pellardo FV, et al. AZT treatment induces molecular and ultrastructural oxidative damage to muscle mitochondria. Prevention by antioxidant vitamins. J Clin Invest 1998;102:4–9.
[8] De la Asuncion JG, del Olmo ML, Sastre J, Pallardo FV, Vina J. Zidovudine (AZT) causes an oxidation of mitochondrial DNA in mouse liver. Hepatology 1999;29:985–7.
[9] Szabados E, Fisher GM, Toth K, Csete B, Nemeti B, Trombitas K, et al. Role of reactive oxygen species and poly-ADP-ribose polymerase in the development of AZT-induced cardiomyopathy in rat. Free Rad Biol Med 1999;314:309–17.
[10] Lenaz G. The mitochondrial production of reactive oxygen species: mechanisms and implications in human pathology. IUBMB Life 2001;52:159–64.
[11] Digirolamo M, Fine JB, Tagra K, Rossmanith R. Qualitative regional differences in adipose tissue growth and cellularity in male Wistar rats fed ad libitum. Am J Physiol 1998;274:R1460–7.
[12] Chiou WL, Ma C, Chung SM, Wu TC, Jeong HY. Similarity in the linear and non-linear oral absorption of drugs between human and rat. Int J Clin Pharmacol Ther 2000;38:532–9.
[13] Freyssenet D, DiCarlo M, Escobar P, Grey J, Schneider J, Hood DA. Zidovudine (AZT) induced alterations in mitochondrial biogenesis in rat striated muscles. Can J Physiol Pharmacol 1999;77:29–35.
[14] Corcuera T, Alonso MJ, Picazo A, Gomez F, Roldan M, Abad M, et al. Hepatic morphological alterations induced by zidovudine (ZDV) in an experimental model. Pathol Res Pract 1996;192:182–7.
[15] Bergenmeyer HU. Methods in enzymatic analysis, vol. VI and VIII, 3rd ed. Verlag Chemie Weinhein, New York, San Francisco, London: Academic Press; 1986.
[16] Klingenberg M, Slenczka W. Pyridine nucleotide in liver mitochondria. An analysis of their redox relationships. Biochem Z 1959;331:486–517.
[17] Srere PA. Citrate synthase. Methods Enzymol 1969;13:3–11.
[18] Rustin P, Chretien D, Bourgeron T, Gérard B, Rötig A, Saudubray JM, et al. Biochemical and molecular investigations in respiratory chain deficiencies. Clin Chim Acta 1994;228:35–51.
[19] Tang PH, Miles VM, DeGrauw A, Hershey A, Pesce A. HPLC analysis of reduced and oxidized coenzyme Q10 in human plasma. Clin Chem 2001;47:256–65.
[20] Marklund S, Marklund G. Involvement of the superoxyde anion radical in the autoxidation of pyrogallol and a convenient assay for superoxide dismutase. Eur J Biochem 1974;47:469–74.
[21] Clairborne Al. In: Grenwald RA, editor. Catalase activity in handbook of methods for oxygen radical research. CRC Press; 1985. p. 283–4.
[22] Günzler WA, Kremers H, Flohe L. An improved coupled test procedure for glutathione peroxidase (EC 1-11-1-9-) in blood. Z klin Chem Klin Biochem 1974;12:444–8.

[23] Melnyk S, Pogribna M, Pogribny I, Hine RJ, James SJ. A new HPLC method for the simultaneous determination of oxidized and reduced plasma aminothiols using coulometric electrochemical detection. J Nutr Biochem 1999;10:490–7.
[24] Speek AJ, Schrijver J, Schreurs WH. Fluorimetric determination of total Vitamin C in whole blood by high-performance liquid chromatography with pre-column derivatization. J Chromatogr 1984;305:53–60.
[25] Yagi K. Lipid peroxydation. Assay for blood plasma or serum. Methods Enzymol 1984;105:328–31.
[26] Labarca C, Paigen K. A simple, rapid, and sensitive DNA assay procedure. Anal Biochem 1980;102:344–52.
[27] Hasegawa T, Juni K, Saneyoshi M, Kawaguchi T. Intestinal absorption and first-pass elimination of 2′,3′-dideoxynucleosides following oral adminstration in rats. Biol Pharm Bull 1996;19:599–603.
[28] Williamson DH, Lund P, Krebs HA. The redox state of free nicotinamide-adenine dinucleotide in the cytoplasm and mitochondria of rat liver. Biochem J 1967;103:514–27.
[29] Deveaud C, Beauvoit B, Salin B, Schaeffer J, Rigoulet M. Regional differences in oxidative capacity of rat white adipose tissue are linked to the mitochondrial content of mature adipocytes. Mol Cell Biochem 2004;267:157–66.
[30] Gaou I, Malliti M, Guimont MC, Letteron P, Demeilliers C, Peytavin G, et al. Effect of stavudine on mitochondrial genome and fatty acid oxidation in lean and obese mice. J Pharmacol Exp Ther 2001;297:516–23.
[31] Ozawa K, Chance B, Tanaka A, Iwata S, Kitai T, Ikai I. Linear correlation between acetoacetate/beta-hydroxybutyrate in arterial blood and oxidized flavoprotein/reduced pyridine nucleotide in freeze-trapped human liver tissue. Biochim Biophys Acta 1992;1138:350–2.
[32] Hassan HM, Fridovich I. Intracellular production of superoxide radical and of hydrogen peroxide by redox active compounds. Arch Biochem Biophys 1979;196:385–95.
[33] Fliers E, Sauerwein HP, Romijn JA, Reiss P, Van der Valk M, Kalsbeek A, et al. HIV-associated adipose redistribution syndrome as a selective autonomic neuropathy. Lancet 2003;362:1758–60.
[34] Giusti V, Suter M, Verdumo C, Gaillard RC, Burckhardt P, Pralong FP. Molecular determinants of human adipose tissue: differences between visceral and subcutaneous compartments in obese women. J Clin Endocrinol Metab 2004;89:1379–84.
[35] Shikuma CM, Hu N, Milne C, Yost F, Waslien C, Shimizu S, et al. Mitochondrial DNA decrease in subcutaneous adipose tissue of HIV-infected individuals with peripheral lipoatrophy. AIDS 2001;15:1801–9.
[36] Walker UA, Bickel M, Lutke Volksbeck SI, Ketelsen UP, Schofer H, Setzer B, et al. Evidence of nucleoside analogue reverse transcriptase inhibitor-associated genetic and structural defects of mitochondria in adipose tissue of HIV-infected patients. J Acquir Immune Defic Syndr 2002;29:117–21.
[37] Cherry CL, Gahan ME, McArthur JC, Lewin SR, Hoy JF, Wesselingh SL. Exposure to dideoxynucleosides is reflected in lowered mitochondrial DNA in subcutaneous fat. J Acquir Immune Defic Syndr 2002;30:271–7.
[38] Nolan D, Hammond E, James I, McKinnon E, Mallal S. Contribution of nucleoside-analogue reverse transcriptase inhibitor therapy to lipoatrophy from the population to the cellular level. Antivir Ther 2003;8:617–26.
[39] Note R, Maisonneuve C, Letteron P, Peytavin G, Djouadi F, Igoudjil A, et al. Mitochondrial and metabolic effects of nucleoside reverse transcriptase inhibitors (NRTIs) in mice receiving one of five single-and three dual-NRTI treatments. Antimicrob Agents Chemother 2003;47:3384–92.